

Intrinsic rotation produced by ion orbit loss and X-loss

W. M. Stacey, J. A. Boedo, T. E. Evans, B. A. Grierson, and R. J. Groebner

Citation: [Phys. Plasmas](#) **19**, 112503 (2012); doi: 10.1063/1.4768424

View online: <http://dx.doi.org/10.1063/1.4768424>

View Table of Contents: <http://pop.aip.org/resource/1/PHPAEN/v19/i11>

Published by the [American Institute of Physics](#).

Related Articles

Measurements of the fast ion slowing-down times in the HL-2A tokamak and comparison to classical theory
[Phys. Plasmas](#) **19**, 112504 (2012)

Spontaneous healing and growth of locked magnetic island chains in toroidal plasmas
[Phys. Plasmas](#) **19**, 112501 (2012)

Low-frequency linear-mode regimes in the tokamak scrape-off layer
[Phys. Plasmas](#) **19**, 112103 (2012)

Spherical torus equilibria reconstructed by a two-fluid, low-collisionality model
[Phys. Plasmas](#) **19**, 102512 (2012)

Oblique electron-cyclotron-emission radial and phase detector of rotating magnetic islands applied to alignment and modulation of electron-cyclotron-current-drive for neoclassical tearing mode stabilization
[Rev. Sci. Instrum.](#) **83**, 103507 (2012)

Additional information on Phys. Plasmas

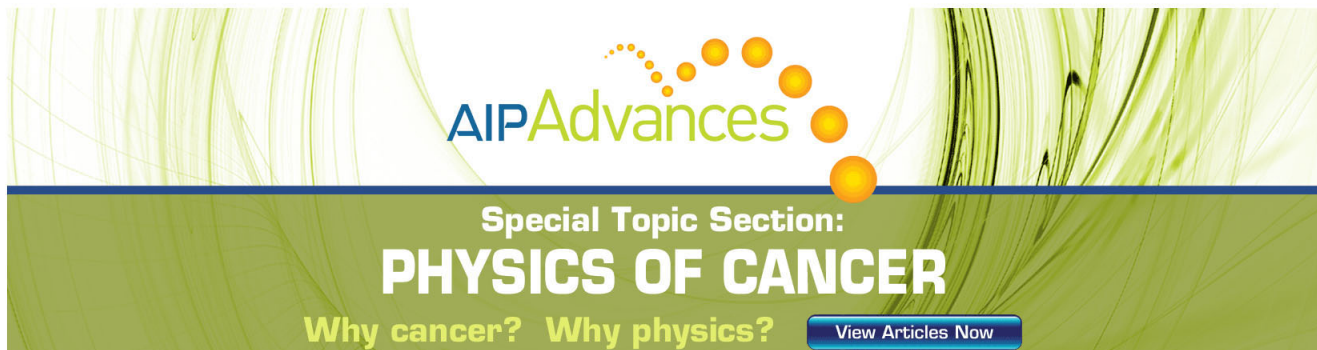
Journal Homepage: <http://pop.aip.org/>

Journal Information: http://pop.aip.org/about/about_the_journal

Top downloads: http://pop.aip.org/features/most_downloaded

Information for Authors: <http://pop.aip.org/authors>

ADVERTISEMENT



AIPAdvances

Special Topic Section:
PHYSICS OF CANCER

Why cancer? Why physics?

[View Articles Now](#)

Intrinsic rotation produced by ion orbit loss and X-loss

W. M. Stacey,¹ J. A. Boedo,² T. E. Evans,³ B. A. Grierson,⁴ and R. J. Groebner³

¹Georgia Institute of Technology, Atlanta, Georgia 30332, USA

²University of California - San Diego, San Diego, California 92093, USA

³General Atomics, San Diego, California 92186, USA

⁴Princeton Plasma Physics Laboratory, Princeton, New Jersey 08453, USA

(Received 10 August 2012; accepted 2 November 2012; published online 26 November 2012)

A practical calculation model for the intrinsic rotation imparted to the edge plasma by the directionally preferential loss of ions on orbits that cross the last closed flux surface is presented and applied to calculate intrinsic rotation in several DIII-D [J. Luxon, *Nucl. Fusion* **42**, 614 (2002)] discharges. The intrinsic rotation produced by ion loss is found to be sensitive to the edge temperature and radial electric field profiles, which has implications for driving intrinsic rotation in future large tokamaks. © 2012 American Institute of Physics. [<http://dx.doi.org/10.1063/1.4768424>]

I. INTRODUCTION

Plasma rotation is important in tokamaks for achieving good confinement,¹ for stabilizing deleterious instabilities,^{2,3} and for triggering the low-high (L-H) confinement transition.⁴ Rotation is driven in present-day tokamaks by neutral beam injection, but in large future tokamaks such as ITER⁵ the momentum input by neutral beam injection will be insufficient to drive present levels of rotation.

It has been observed that tokamak plasmas rotate even in the absence of external momentum injection.^{6–13} There is evidence^{13–15} that the momentum source (or sink) causing this so-called “intrinsic” rotation is located in the edge. Plasma ion orbit loss,^{16,17} turbulence,^{18–21} non-axisymmetric fields,²² viscous coupling to scrape-off layer flows,^{23–25} Reynolds stress,²⁶ and charge-exchange are mechanisms that could cause intrinsic rotation.

This paper describes models for calculation of the intrinsic rotation produced by two ion orbit loss mechanisms of “thermalized” plasma ions. (i) The loss of ions across the last closed flux surface (LCFS) on orbits constrained by canonical angular momentum, energy, and magnetic moment conservation and (ii) the downward (radially outward) grad-B and curvature drift of ions trapped poloidally in the low B_θ region near the X-point. These models for the intrinsic rotation are based on extensions of previous models for the ion orbit loss and X-loss of ions and ion energy.^{27,28} Calculations of intrinsic parallel rotation caused by these ion orbit loss and X-loss mechanisms are compared with measurements in DIII-D²⁹ plasmas.

II. CALCULATION OF ION LOSSES IN THE EDGE PLASMA

We are concerned with the calculation of the loss of plasma ions, their energy, and in particular for this paper their directed momentum by excursions from the flux surface on orbits that cross the LCFS, which we define as lost from the plasma (it is possible, of course, to define other loss surfaces or to calculate return fractions, but this is beyond the scope of the present paper). Such processes take place for the “thermalized” plasma ions primarily in the edge

plasma, which is constantly replenished by outward ion particle, energy, and momentum fluxes from the core plasma. The basic orbit loss processes are “ion orbit loss” described by Miyamoto³⁰ and others and “X-loss” described by Chang and colleagues³¹ and more recently by Stacey.²⁸

We have found^{27,28} that at each flux surface in the plasma edge there is a minimum ion speed $V_{\min(\zeta_0)}$ (or energy) for which an ion with a given directional cosine ζ_0 with respect to the magnetic field can be lost, for both of these processes, and that all ions with a given ζ_0 and speeds above this minimum will be lost. We have also found^{27,28} by numerical calculation for several edge plasma distributions that $V_{\min(\zeta_0)}$ decreases with increasing plasma radius (decreasing distance to the last closed flux surface). As a given volume of plasma flows outward across the plasma edge it first loses the highest energy ions and then loses successively lower energy ions as it flows across successively outward flux surfaces. This loss is different for the different ion directions ζ_0 . So, the “hole” in the plasma velocity distribution extends progressively down to lower $V_{\min(\zeta_0)}$ with increasing radius, and the depth of the “hole” is different for different ζ_0 ; i.e., the loss region is cumulative and directionally dependent.

The ion loss situation for a constant influx of plasma (from the core) flowing across the edge region and accumulating a progressively larger and direction-dependent loss region is different from the situation usually calculated of a static plasma with no source and a fixed loss cone. In the latter static, source-free situation, in-scattering of plasma from outside the loss cone is necessary to maintain the plasma loss rate. However, in the flowing plasma situation considered in this paper, the plasma loss rate is maintained by the influx of plasma from the core into the edge region. We do not consider in-scattering in this paper, based on estimates^{27,28} that it would only slightly increase the calculated loss rates in most DIII-D discharges.

The details of ion particle and energy loss in a plasma flowing across the edge region in a tokamak have been worked out in Refs. 27 and 28, where detailed calculation results may be found. These results are extended in this paper to calculate the net directional momentum loss; hence, the net oppositely directed momentum in the remaining

plasma ions that are not lost (i.e., the intrinsic rotation produced by the directed momentum loss).

III. INTRINSIC ROTATION DUE TO ION ORBIT LOSS

The loss of plasma ions on orbits that cross the LCFS or some other loss surface has been recognized for many years.^{30,32,33} More recently, it has been recognized that the preferential loss of ions with directionality along the magnetic field leaves the plasma with ions preferentially directed in the opposite direction.^{17,18}

The basic ion orbit calculation is of the minimum energy an ion located at a particular position (ψ_0, θ_0) on an internal flux surface with a direction cosine ζ_0 relative to the toroidal magnetic field direction must have in order to be able to execute an orbit that will cross the loss flux surface (which is taken to be the LCFS or separatrix in this paper) at location $(\psi_{sep}, \theta_{sep})$. Following Miyamoto³⁰ and more recently Stacey,²⁷ we make use of the conservation of canonical toroidal angular momentum

$$RmV_{||}f_{\phi} + e\psi = \text{const} = R_0mV_{||0}f_{\phi 0} + e\psi_0, \quad (1)$$

to write the orbit constraint for an ion introduced at a location (ψ_0, θ_0) with parallel velocity $V_{||0}$, where $f_{\phi} = |B_{\phi}/B|$, R is the major radius, and ψ is the flux surface value. The conservation of energy and of magnetic moment

$$\begin{aligned} \frac{1}{2}m(V_{||}^2 + V_{\perp}^2) + e\phi &= \text{const} = \frac{1}{2}m(V_{||0}^2 + V_{\perp 0}^2) + e\phi_0 \\ &\equiv \frac{1}{2}mV_0^2 + e\phi_0 \\ \frac{mV_{\perp}^2}{2B} &= \text{const} = \frac{mV_{\perp 0}^2}{2B_0} \end{aligned} \quad (2)$$

further require that

$$V_{||} = \pm V_0 \left[1 - \left| \frac{B}{B_0} \right| (1 - \zeta_0^2) + \frac{2e}{mV_0^2} (\phi - \phi_0) \right]^{\frac{1}{2}}, \quad (3)$$

where ϕ is the electrostatic potential. The quantity $\zeta_0 = V_{||0}/V_0$ is the cosine of the initial guiding center velocity relative to the magnetic field direction. Using Eqs. (3) in (1) and squaring leads to a quadratic equation in the initial ion velocity $V_0 = \sqrt{V_{||0}^2 + V_{\perp 0}^2}$.

$$\begin{aligned} V_0^2 \left[\left(\left| \frac{B}{B_0} \right| \frac{f_{\phi 0} \zeta_0}{f_{\phi}} \right)^2 - 1 + (1 - \zeta_0^2) \left| \frac{B}{B_0} \right| \right] \\ + V_0 \left[\frac{2e(\psi_0 - \psi)}{Rmf_{\phi}} \left(\left| \frac{B}{B_0} \right| \frac{f_{\phi 0} \zeta_0}{f_{\phi}} \right) \right] \\ + \left[\left(\frac{e(\psi_0 - \psi)}{Rmf_{\phi}} \right)^2 - \frac{2e(\phi_0 - \phi)}{m} \right] = 0. \end{aligned} \quad (4)$$

Note that Eq. (4) is quite general with respect to the flux surface geometry representation of R , B , and the flux surfaces ψ .

By specifying an initial “0” location for an ion with initial direction cosine with respect to \mathbf{B} , denoted ζ_0 , and specifying a final location on flux surface ψ , Eq. (4) can be solved to determine the minimum initial ion speed V_0 that is required in order for the ion orbit to reach the final location. Thus, Eq. (4) can be solved for the minimum ion speed or energy necessary for an ion located at some point on an internal flux surface, with a given ζ_0 , to cross the last closed flux surface ψ_{sep} (or any other “loss” flux surface) at a given location θ_{sep} (or to strike the chamber wall at a given location, $(\psi_{wall}, \theta_{wall})$, etc.). A minimum reduced energy for ion orbit loss $\varepsilon_{\min}(\rho, \zeta_0) \equiv 1/2mV_{0\min}^2(\rho, \zeta_0)/kT_{ion}(\rho)$ can thus be calculated for each location on the flux surface designated by ρ , for each value of the direction cosine.²⁷

Such calculations of minimum speeds required for ions with different values of the direction cosine at different poloidal locations on internal flux surfaces to cross the LCFS at various poloidal locations can be carried out straightforwardly.²⁷ Note in this regard that it is the values of the flux surfaces and of the electrostatic potential, ion temperature, magnetic field, and major radius on these flux surfaces that are important for the calculation, not the location of the flux surface in Euclidian space per se. We use the fraction of the magnetic flux enclosed to define ρ , which should allow an accurate mapping of the experimental parameters to flux surfaces. This result encourages the use of a simple approximate circular flux surface model that conserves flux surface area and enclosed current for the calculations for the general ion orbit loss calculation, the principle geometric approximation of which is that $RB_{\phi} = \text{const.}$ over the plasma.

We consider a tokamak configuration in which the toroidal current and the toroidal magnetic field are oppositely directed. In such a configuration the usual (but not always) preferential loss of $\zeta_0 > 0$ (counter-current) ions causes a residual $\zeta_0 < 0$ (co-current) intrinsic rotation in the edge plasma due to the preferential retention of co-current directed ion orbit loss that has taken place over all inner radii out to that flux surface. Assuming, for computational simplification, an initially Maxwellian distribution of the plasma influx at innermost radius of the computation and determining the minimum loss speed $V_{\min}(\zeta_0)$ as described above leads to an expression for the net parallel momentum loss (when multiplied by nm)

$$\begin{aligned} \Delta V_{||}(\rho) &= 2\pi \int_{-1}^1 d\zeta_0 \left[\int_{V_{\min}(\zeta_0)}^{\infty} (V_0 \zeta_0) V_0^2 f(V_0) dV_0 \right]_{\rho} \\ &= 4\pi M_{orb}(\rho) \left[\int_0^{\infty} (V_0) V_0^2 f(V_0) dV_0 \right]_{\rho} \\ &= 2 \frac{\Gamma(2)}{\pi^{\frac{1}{2}}} M_{orb}(\rho) V_{th}(\rho) = \frac{2}{\pi^{\frac{1}{2}}} M_{orb}(\rho) \sqrt{\frac{2kT_{ion}(\rho)}{m}}, \end{aligned} \quad (5)$$

where

$$\begin{aligned}
M_{orb}(\rho) &\equiv \frac{M_{loss}}{M_{tot}} = \frac{\int_{-1}^1 \left[\int_{V_{0min}(\zeta_0)}^{\infty} (mV_0\zeta_0)V_0^2 f(V_0) dV_0 \right] d\zeta_0}{2 \int_0^{\infty} (mV_0)V_0^2 f(V_0) dV_0} \\
&= \frac{\int_{-1}^1 \zeta_0 \Gamma(2, \varepsilon_{min}(\rho, \zeta_0)) d\zeta_0}{2\Gamma(2)}. \quad (6)
\end{aligned}$$

Here $\Gamma(n)$ and $\Gamma(n, x)$ are the gamma and incomplete gamma functions and M_{orb} is the net parallel momentum loss fraction. Equation (5) usually defines a net counter-current parallel velocity loss, which produces a net co-current intrinsic rotation of the remaining ions in the plasma edge, for the configuration being considered in which the toroidal current and magnetic field are oppositely directed.

Note that the direction cosine under the integrals in the numerators in Eqs. (5) and (6) weight counter-current losses positive and co-current negative, so the net result depends on the minimum loss speed for the various values of the direction cosine, which is determined by solving Eq. (4) for a given ion location on an interior flux surface. The lowest loss speeds that will allow a particle to cross the separatrix at any point are determined for various “launch points” on the interior flux surface, as discussed in Ref. 27. Then, assuming that ions can move freely over the flux surface, the lowest of these minimum speeds is taken as the minimum speed for the flux surface for the purpose of evaluating Eq. (5) (taking the average, instead of the lowest, minimum loss energy does not much affect the results).

Since $M_{orb} \ll 1$, usually $\Delta V_{\parallel} \ll V_{th}$, but as we shall see it can be significant.

The ion orbit loss will be different for the main deuterium (D) ions and for the usual carbon (C) impurity ions. While the ion mass and charge enter Eq. (4) for $V_{min}(\zeta_0)$ as the ratio e/m , which is the same for C and D, so that $V_{min}(\zeta_0)$ is the same for C and D, $\varepsilon_{min}(\zeta_0) \equiv 1/2mV_{min}^2(\zeta_0)/kT_{ion}$ is 6 times larger for C than D, which means that $\Gamma(2, \varepsilon_{min}) = \int_{\varepsilon_{min}}^{\infty} \varepsilon e^{-\varepsilon} d\varepsilon$ is smaller for C than for D (i.e., the fraction of the ions that can escape, M_{orb} , is also smaller for C than for D). Taking into account that $V_{th}^D/V_{th}^C = \sqrt{6}$ in the formula for the intrinsic velocity due to ion orbit loss, $\Delta V_{\parallel} \approx M_{orb}V_{th}$, it is clear that $\Delta V_{\parallel}^D > 2.5\Delta V_{\parallel}^C$ because of the additional difference in M_{orb} between carbon and deuterium associated with the difference in ε_{min} .

Because a similar loss mechanism does not exist for the much smaller mass electrons, ion orbit loss would tend build up a net charge in the plasma unless compensated by a current of ions or electrons caused by another mechanism. Since the ion orbit loss is a radially distributed loss of charge which must be balanced by the divergence of the compensating current flowing radially in the plasma, the radial electric field would adjust to maintain force balance. By using the experimental values of the radial electric field in the calculations of this paper, we indirectly take into account the effect of this compensating current, but a first-principles calculation would require taking these compensating currents into account in the calculation of the radial electric field.

We note that deGrassie also has developed¹⁷ an ion orbit loss model for intrinsic rotation based on the same basic principles of conservation of canonical angular momentum, energy, and magnetic moment, but involving a different computational methodology. His model predicted intrinsic rotation in relatively good agreement with measurements in DIII-D.³⁴

IV. INTRINSIC ROTATION DUE TO X-LOSS OF IONS

There is a different type of ion orbit loss near the X-point in diverted plasmas.^{28,31} In a region about the X-point the poloidal field is very small, $B_{\theta} \ll \varepsilon B_{\phi}$, and the field lines are almost purely toroidal and do not spiral about the tokamak to provide the usual neoclassical cancellation of drift effects. However, ions quite rapidly move poloidally over the remainder of the flux surface outside of this “X-region” by following along spiraling field lines. As the ions approach the X-point their poloidal motion is provided only by the slower poloidal $E_r \times B_{\phi}$ drift due to the radial electric field. If the ion poloidal spiral direction about the field lines in the plasma is the same as the $E_r \times B_{\phi}$ drift direction into the x-region, ions will move poloidally into and across the null- B_{θ} region near the X-point until they enter a plasma region in which $B_{\theta} \approx \varepsilon B_{\phi}$ once again, in which they can rapidly move poloidally over the flux surface by following the spiraling motion of the field lines. Since particles are swept poloidally over the flux surface in a time that is short compared to the time for significant radial flow, they are repetitively swept into and out of this X-region if they are spiraling in a direction for which the $E_r \times B_{\phi}$ drift is into the X-region.

However, while the ions are slowly drifting poloidally across the null- B_{θ} X-region near the X-point, they are also drifting vertically due to curvature and grad-B drifts. In the configuration considered in this paper, with the toroidal field in the clockwise direction (looking down from above) and the plasma current in the counter-clockwise direction, this vertical drift would be downward towards a lower single-null divertor. If the time required for the ion to grad-B and curvature drift downward across the LCFS is less than the time required for the ion to $E_r \times B_{\phi}$ drift across the $B_{\theta} \ll \varepsilon B_{\phi}$ X-region near the X-point, the ion will be lost across the LCFS. Even if the ion is not lost across the LCFS, it will be displaced radially outward while it is traversing the null- B_{θ} region; i.e., it will be X-transported.²⁸

The time required for an ion entering the X-region at radius r to grad-B and curvature drift downward a distance Δr is

$$\tau_{\nabla B} = \frac{\Delta r}{V_{\nabla B,c}} = \frac{\Delta r}{(W_{\perp} + 2W_{\parallel})/eRB} = \frac{eRB}{W(1 + \zeta_0^2)} \Delta r, \quad (7)$$

where ζ_0 is the cosine of ion direction with respect to the magnetic field and W denotes the ion energy. During this time the ion is also $E_r \times B_{\phi}$ drifting through a poloidal arc distance

$$r\Delta\theta = V_{E \times B} \tau_{\nabla B} = \frac{E_r(r)}{B_{\phi}} \frac{eRB}{W(1 + \zeta_0^2)} \Delta r. \quad (8)$$

If the radial distance from the location at which the ion enters the X-region is sufficiently short that the ion can grad-B and curvature drift radially downward before it $E_r \times B_\phi$ drifts across the angular extent $\Delta\theta_x$ of the X-region (see Ref. 28 for a description of geometry) and re-enters the plasma, the ion and any parallel momentum that it has will be X-lost from the plasma into the private flux region. The minimum energy for which an ion entering the X-region at a given radius with a given direction cosine can be X-lost across the LCFS can be calculated numerically,^{27,28} taking into account the radial dependence of E_r and T_i . In the configuration considered in this paper (looking down-clockwise B_ϕ , counter-clockwise I_ϕ) ions with $\zeta_0 \equiv (\mathbf{V} \cdot \mathbf{B})/(VB) > 0$ that will spiral towards the X-region in such a direction that the $E_r \times B_\phi$ drift will carry the ion into the X-region, but ions with $\zeta_0 < 0$ will not enter the X-region. This imparts a strong directionality to the X-loss which results in an intrinsic current.

For the configuration considered in this paper, the net fraction of ion parallel momentum at a given radius that enters the X-region and is X-lost is

$$M_x(\rho) \equiv \frac{M_{loss}}{M_{tot}} = \frac{\int_0^1 \left[\int_{V_{Xmin}(\zeta_0)}^\infty (mV_0\zeta_0)V_0^2 f(V_0) dV_0 \right] d\zeta_0}{2 \int_0^\infty (mV_0)V_0^2 f(V_0) dV_0} = \frac{\int_0^1 \zeta_0 \Gamma(2, \varepsilon_{Xmin}(\zeta_0)(\rho)) d\zeta_0}{2\Gamma(2)}, \quad (9)$$

where $V_{Xmin}(\zeta_0) = \sqrt{2W_{Xmin}(\zeta_0)/m}$ is determined numerically as described above, and the reduced energy is $\varepsilon_{Xmin}(\zeta_0) = W_{Xmin}(\zeta_0)/kT$. The lost ions are all counter-current directed, in the configuration considered, resulting in a net co-current intrinsic rotation

$$\begin{aligned} \Delta V_{||}(\rho) &= 2\pi \int_0^1 d\zeta_0 \left[\int_{V_{Xmin}(\zeta_0)}^\infty (V_0\zeta_0)V_0^2 f(V_0) dV_0 \right]_\rho \\ &= 4\pi M_{orb}(\rho) \left[\int_0^\infty (V_0)V_0^2 f(V_0) dV_0 \right]_\rho \\ &= 2 \frac{\Gamma(2)}{\pi^{1/2}} M_x(\rho) V_{th}(\rho) = \frac{2}{\pi^{1/2}} M_x(\rho) \sqrt{\frac{2kT_{ion}(\rho)}{m}}. \end{aligned} \quad (10)$$

Carbon ions will be X-lost at a different rate than deuterium ions. It is clear from Eq. (7) that the minimum loss energies are related as $W_{Xmin}^C \simeq 6W_{Xmin}^D$, so that a larger fraction of the deuterium ions will be X-lost, $M_X^C < M_X^D$. Further taking into account the mass dependence of V_{th} , it is clear from Eq. (10) that $\Delta V_{||}^D > 2.5\Delta V_{||}^C$ because of the additional difference in M_x between carbon and deuterium associated with the difference in ε_{Xmin} .

Electrons drifting into the X-region would of course have grad-B and curvature drifts in the direction opposite to the ion drifts. The net current due to X-transport of ions and

electrons has not been worked out. However, by using the experimental radial electric fields, we should be taking into account the effects of the compensating currents needed to maintain charge neutrality.

V. APPLICATIONS TO DIII-D

In this section several applications of the above theoretical model to interpret intrinsic rotation in the DIII-D tokamak²⁹ are described.

A. Ohmic discharges 146598 and 146600

We first examine the early ohmic phase of two similar discharges in which Mach probe measurements of the parallel rotation of D ions and CER measurements of the parallel rotation of C ions were made in the edge plasma,³⁵ discharges 146598 and 146600, both with similar parameters ($R=1.734$ m, $a=0.583$ m, $\kappa=1.727$, $B=-1.649$ T, $I=0.93$ MA), but slight differences in geometry. In both discharges, the configuration was with the current counter-clockwise looking down on the tokamak, the magnetic field oppositely directed, and a lower single null divertor. The main plasma parameters for the ion orbit loss and X-loss calculation, the ion temperature, and the radial electric field (which can be integrated to obtain the electrostatic potential) are given in Figs. 1 and 2.

We use an effective circular model of the plasma that conserves the flux surface area and further assume a uniform current density to obtain flux surfaces $\psi(\rho) \sim I\rho^2$ which are used, together with the data in Figs. 1 and 2, to calculate the intrinsic rotation due to ion orbit loss from the formalism of Sec. III. Then the effect of the divertor is treated separately by calculating the X-loss, using the formalism of Sec. IV. The intrinsic rotation of deuterium and carbon ions due to ion orbit loss, as calculated with Eqs. (1)–(6), and the intrinsic rotation due to the X-loss of deuterium ions, as calculated with Eqs. (7)–(10), are shown in Fig. 3.

There was a small external momentum input due to neutral beam “blips” in both discharges, but these were after the probe measurements, and the C^{+6} measurements were made

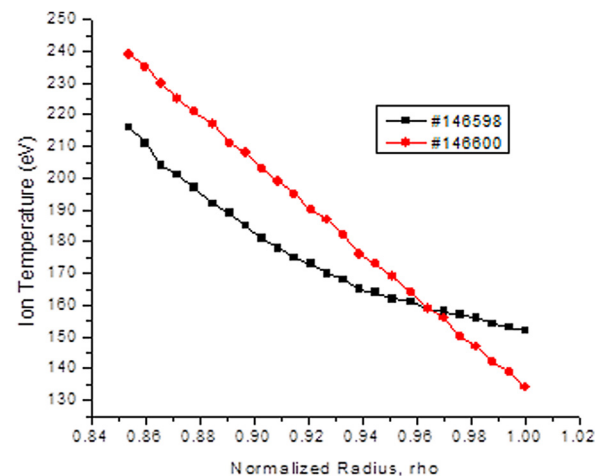


FIG. 1. Measured ion temperature distributions in DIII-D discharges 146598 and 146600 at 1105 ms (data will be described in detail in Ref. 35).

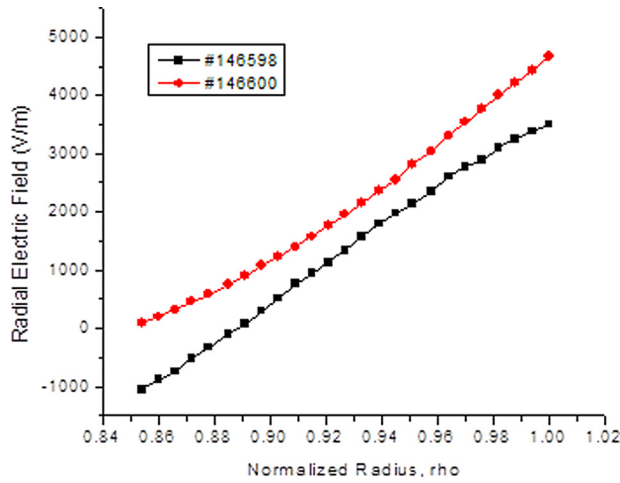


FIG. 2. Measured radial electric field distributions in DIII-D discharges 146598 and 146600 at 1105 ms (data will be described in detail in Ref. 35).

within a few ms of the first blips, so it is unlikely that the blips had any significant torque effect upon the measured rotation. The measured rotation generally peaked at mid-radius then decreased with radius towards the edge, but then increased sharply with radius just inside the separatrix, in both discharges, as shown in Figs. 4 and 5. These increases in measured co-current rotation just inside the separatrix are comparable in magnitude and direction to the net ion orbit loss sink of predominantly counter-current ions in the plasma edge just inside the separatrix, which would produce a net co-current rotation in the remaining ions.

The measured (probes) D rotation decreased with radius in the plasma edge out to about 20 km/s at $\rho = 0.98$ and then increased sharply to about 30 km/s at $\rho = 0.99$ and about 40 km/s at $\rho = 1.0$. The ion orbit loss calculation of Eq. (5) predicted net co-current deuterium velocities of about 12 km/s at $\rho = 0.982$ increasing sharply to about 25 km/s at $\rho = 0.994$.

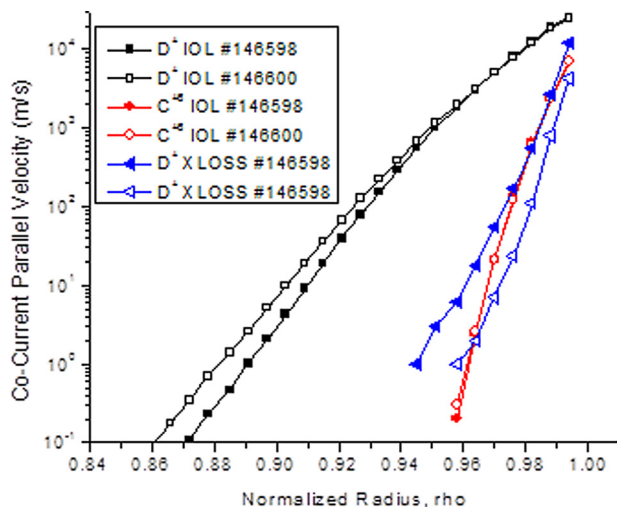


FIG. 3. Calculated intrinsic rotation velocities for ion orbit loss from Eq. (5) and for X-loss from Eq. (10) for DIII-D ohmic discharges 146598 and 146600. ("C⁺" and "D" indicate carbon+6 and deuterium; "IOL" and "XLOSS" indicate the ion orbit loss and X-loss calculations of Secs. III and IV).

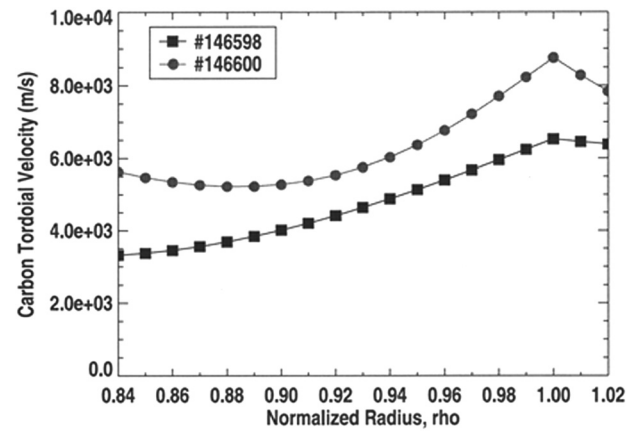


FIG. 4. Carbon toroidal velocity measured (CER) in the plasma edge of ohmic DIII-D shots.

The CER (charge-exchange and recombination) measured C⁺ rotation exhibited a similar behavior but with smaller magnitude, about 5–7 km/s at $\rho = 0.98$ and then increasing to about 6–8 km/s at $\rho = 0.99$ and 6–9 km/s at $\rho = 1.0$. The ion orbit loss calculation predicted net co-current carbon velocities, about 0.6 km/s at $\rho = 0.982$ increasing sharply to about 7 km/s at $\rho = 0.994$, which are similar to the measured values just inside the separatrix.

The measured deuterium and carbon rotation velocities differed by about a factor of 5 just inside the separatrix, while the ion orbit loss calculation predicted a difference of about a factor of 3.6.

The evaluation of the minimum energy for X-loss is sensitive to the angular width of the X-region. Based on magnetic field contours for the H-mode DIII-D shot^{36–38} discussed next, a value of the angular width of the X-loss region $\Delta\theta_x = 0.15$ radians was estimated. Using this value of $\Delta\theta_x = 0.15$ and a larger value $\Delta\theta_x = 0.25$, intrinsic rotation due to X-loss was calculated to be 12 and 17 km/s, respectively, at $\rho = 0.994$ and of 2.6 and 8.4 km/s at $\rho = 0.988$.

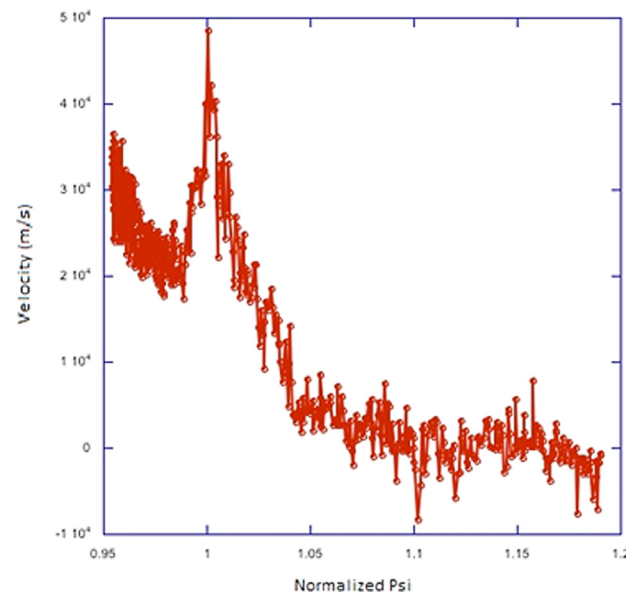


FIG. 5. Mach-probe measurement of deuterium parallel velocity in DIII-D ohmic shot 146598.

The $\Delta\theta_x = 0.15$ calculation is shown in Fig. 3. These values of intrinsic rotation due to X-loss are smaller than the values of intrinsic rotation due to ion orbit loss, and the two processes involve ions in similar energy ranges (which cannot be lost twice), so the larger losses due to ion orbit loss are considered to be representative of the losses due to both processes for these two discharges.

B. Matched ELMing H-mode discharge 123302 and resonance magnetic perturbation (RMP) discharge 123301

The DIII-D ELMing (Edge Localized Mode) H-mode discharge 123302 and the otherwise similar discharge 123301 (Refs. 36–38) with RMP coils ($R = 1.746$ m, $a = 0.599$ m, $\kappa = 1.836$, $B = -2.0$ T, $I = 1.5$ MA, $P_{NB} = 8.7$ MW) have been extensively analysed^{36–38} and were chosen to illustrate the magnitude of intrinsic rotation due to ion orbit loss and X-loss that would be predicted for a typical H-mode discharge and for a similar discharge that has quite different ion temperature and radial electric field structure in the plasma edge, as shown in Figs. 6 and 7. Both of these discharges were strongly rotating in the co-current direction due to neutral beam injection. These discharges had the “standard” DIII-D configuration of a clockwise magnetic field and a counter-clockwise current, looking down on the tokamak, and a lower single null divertor.

The intrinsic rotation due to ion orbit loss was calculated using Eqs. (1)–(6) and the data of Figs. 6 and 7, for both the deuterium and carbon impurity ions, and the intrinsic rotation due to X-loss was calculated using Eqs. (6)–(10) for the deuterium ions. The momentum loss was preferentially of ions with directions counter to the plasma current, as illustrated in Fig. 8 by the calculated fractional parallel momentum loss rate (the integrand in the last form of Eq. (6)). This preferential loss of counter-current momentum left the plasma with a net co-current intrinsic rotation, as shown in Fig. 9. Comparing the intrinsic carbon velocity due to ion orbit loss with the CER measurement of carbon toroidal rotation, it is clear that the predicted intrinsic carbon rotation is a

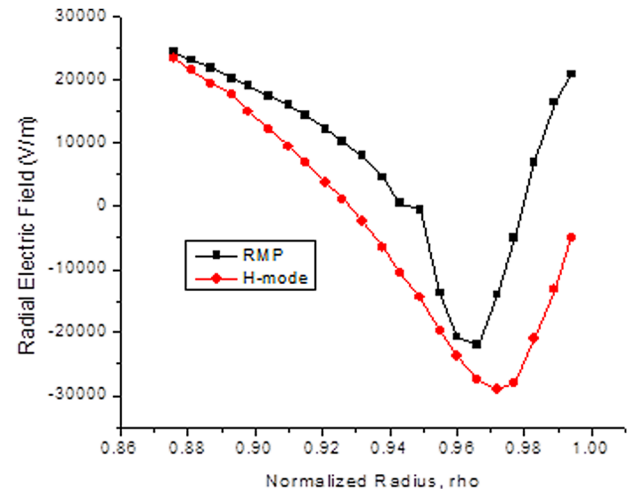


FIG. 7. Measured radial electric field distributions in matched ELMing H-mode discharge 123302 and RMP discharge 123301 at 2600 ms (data are described in Refs. 36–38).

small fraction of the total carbon toroidal rotation driven by the neutral beams, except just inside the separatrix where the two become comparable. On the other hand, the predicted intrinsic rotation due to ion orbit loss for deuterium is comparable to the measured carbon rotation over a significant fraction of the edge plasma.

The predicted deuterium intrinsic rotation due to ion orbit loss is much larger in the RMP discharge than in the H-mode discharge. This is due to the hotter RMP discharge having a larger population of higher energy ions that can access loss orbits than the H-mode discharge and to the differences in the electric field structure.

The deuterium intrinsic rotation due to X-loss is predominantly located just inside the separatrix for the H-mode discharge, but there is a large intrinsic rotation due to X-loss predicted from radii around $\rho \approx 0.95$ for the RMP discharge. At the same time, for the RMP discharge there is a gap between $\rho \approx 0.96$ and $\rho \approx 0.98$ in which there is no intrinsic

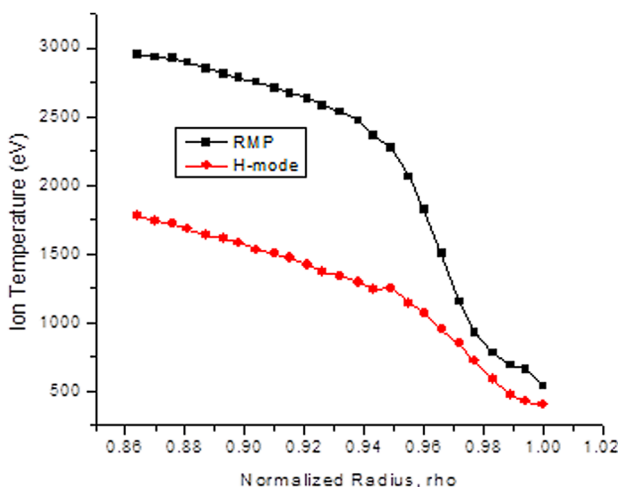


FIG. 6. Measured ion temperature distributions in matched ELMing H-mode discharge 123302 and RMP discharge 123301 at 2600 ms (data are described in Refs. 36–38).

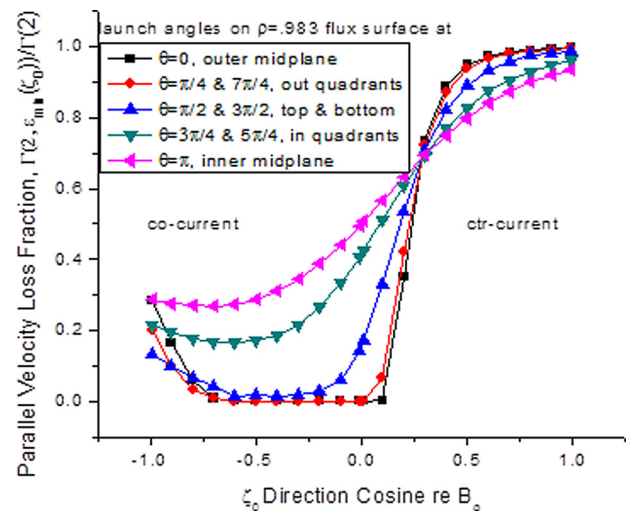


FIG. 8. Directional dependence of the parallel velocity ion orbit loss fraction from several locations on the $\rho = 0.983$ flux surface for H-mode discharge 123302.

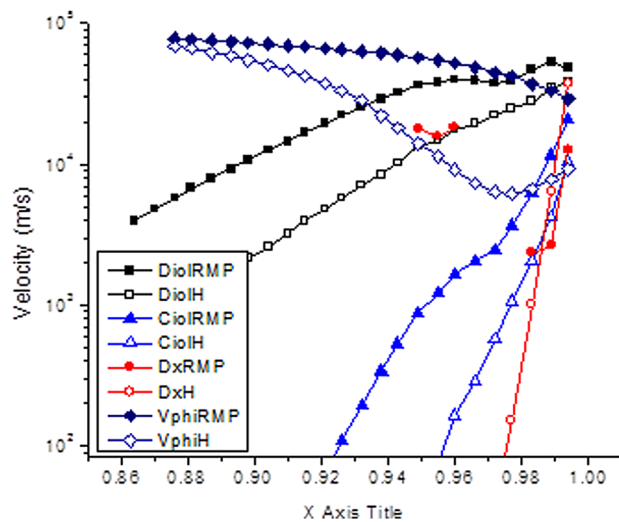


FIG. 9. Calculated intrinsic rotation due to ion orbit loss and X-loss in matched ELMy H-mode discharge 123302 and RMP discharge 123301 at 2600 ms (“C” and “D” indicate carbon+6 and deuterium; “iol” and “x” indicate the ion orbit loss and X-loss calculations of Secs. III and IV; “H” and “RMP” refer to H-mode and resonance-magnetic-perturbation; “Vphi” is the CER measured toroidal velocity for carbon+6).

rotation because ions entering the X-region in that interval cannot be X-loss at any reasonable energy because of the radial structure of the electric field in the RMP discharge.

C. Geometry dependence

The above considerations have been worked out for a “standard” DIII-D lower single null divertor configuration with the magnetic field in the clockwise direction and the current in the counter-clockwise direction, looking down on the tokamak. For this configuration the grad-B and curvature ion drifts are downward into the divertor and the ctr-current particles with $\zeta_0 > 0$ have orbits outside the flux surface that are preferentially lost by ion orbit loss and drift down and outward into the divertor when trapped in the x-region, both processes creating co-current intrinsic rotation. If the magnetic field were to be reversed to be parallel with the current in the counter-clockwise direction looking down on the tokamak, then the grad-B and curvature ion drifts would be upward, which should shut off the x-loss mechanism for a lower divertor, but it is still the ctr-current particles (but now with $\zeta_0 < 0$) that have orbits outside the flux surface that are preferentially lost, producing an intrinsic co-current. If an upper divertor replaced the lower divertor then the upward grad-B and curvature drifts would again be outward and the X-loss mechanism would be turned back on for the parallel counter-clockwise current and field configuration.

VI. SUMMARY AND CONCLUSIONS

The preferential directionality of the loss of ions from interior flux surfaces by executing orbits that cross the last closed flux surface (or any other exterior loss surface) causes the remaining ions in the plasma to be predominantly of the opposite directionality, which constitutes an intrinsic plasma rotation in that direction. In the “standard configuration”

DIII-D discharges considered, with the current counter-clockwise and the magnetic field clockwise (looking down from above), the resulting intrinsic rotation is co-current. A calculation model for this intrinsic rotation was described, and some applications to calculate intrinsic rotation in DIII-D discharges were presented. The magnitudes of the intrinsic rotation predictions just inside the separatrix were similar to those observed in DIII-D ohmic discharges. They were also of sufficient magnitude in beam-heated discharges that they should be taken into account in comparisons of rotation theories with measurements in the edge plasma, certainly in DIII-D and probably in other strongly rotating experiments as well.

Some interesting relationships between the radial electric field and the intrinsic rotation were found. This raises the possibility of generating intrinsic rotation by controlling the electric field in the edge plasma, which could be useful in future tokamaks such as ITER.

ACKNOWLEDGMENTS

The first author is grateful to John deGrassie for a couple of useful discussions on the subject and to General Atomics for their hospitality during the course of some of the work reported in this paper. The contributions of other members of the DIII-D Team are gratefully acknowledged. This work was supported by the U. S. Department of Energy through Grant No. DE-FG02-99ER54538 with the Georgia Tech Research Corporation and through Contract No. DE-AC03-99ER54463 with General Atomics.

- ¹P. A. Politzer, C. C. Petty, R. J. Jayakumar, T. C. Luce, M. R. Wade, J. C. deBoo, J. R. Ferron, P. Gohil, C. T. Holcomb, A. W. Hyatt, J. Kinsey, R. J. La Haye, M. A. Makowski, and T. W. Petrie, *Nucl. Fusion* **48**, 075001 (2008).
- ²R. J. Buttery, R. J. La Haye, P. Gohil, G. L. Jackson, H. Reimerdes, and E. J. Strait, *Phys. Plasmas* **15**, 056115 (2008).
- ³A. M. Garofalo, G. L. Jackson, F. J. La Haye, M. Okabayashi, H. Reimerdes, E. J. Strait, J. R. Ferron, R. J. Groebner, Y. In, M. J. Lancot, G. Matsunaga, G. A. Navratil, W. M. Solomon, H. Takahashi, M. Takechi, A. D. Turnbull, and DIII-D Team, *Nucl. Fusion* **47**, 1121 (2007).
- ⁴G. R. McKee, P. Gohil, D. J. Schlossberg, J. A. Boedo, K. H. Burrell, J. S. deGrassie, R. J. Groebner, R. A. Moyer, C. C. Petty, T. L. Rhodes, L. Schmitz, M. W. Shafer, W. M. Solomon, M. Umansky, G. Wang, A. E. White, and X. Xu, *Nucl. Fusion* **49**, 115016 (2009).
- ⁵See www.iter.org for information about ITER.
- ⁶J. E. Rice, M. Greenwald, I. H. Hutchinson, E. S. Marmar, Y. Takase, S. M. Wolfe, and F. Bombarda, *Nucl. Fusion* **38**, 75 (1998).
- ⁷L. G. Erickson, E. Righi, and K.-D. Zastrow, *Plasma Phys. Controlled Fusion* **39**, 27 (1977).
- ⁸I. H. Hutchinson, J. E. Rice, R. S. Granetz, and J. A. Snipes, *Phys. Rev. Lett.* **84**, 3330 (2000).
- ⁹B. P. Duval, A. Bortolon, A. Karpushov, R. A. Pitts, A. Pochelon, O. Sauter, A. Scarabosio, and G. Turri, *Phys. Plasmas* **15**, 056113 (2008).
- ¹⁰J. E. Rice, A. Ince-Cushman, J. S. deGrassie, L.-G. Eriksson, Y. Sakamoto, A. Scarabosio, A. Bortolon, K. H. Burrell, B. P. Duval, C. Genzi-Bonizic, M. J. Greenwald, R. J. Groebner, G. T. Hoang, Y. Koide, E. S. Marmar, A. Pochelon, and Y. Podpaly, *Nucl. Fusion* **47**, 1618 (2007).
- ¹¹S. H. Mueller *et al.*, *Phys. Rev. Lett.* **106**, 115001 (2011).
- ¹²S. H. Mueller *et al.*, *Phys. Plasmas* **18**, 072504 (2011).
- ¹³J. A. Boedo, E. A. Belli, E. Hollmann, W. M. Solomon, D. L. Rudakov, J. G. Watkins, R. Prater, J. Candy, R. J. Groebner, K. H. Burrell, J. S. deGrassie, C. J. Lasnier, A. W. Leonard, R. A. Moyer, G. D. Porter, N. H. Brooks, S. Muller, G. Tynan, and E. A. Unterberg, *Phys. Plasmas* **18**, 032510 (2011).

- ¹⁴W. D. Lee, J. E. Rice, E. S. Marmor, M. J. Greenwald, I. H. Hutchinson, and J. A. Snipes, *Phys. Rev. Lett.* **91**, 205003 (2003).
- ¹⁵W. M. Solomon, K. H. Burrell, A. M. Garofalo, A. J. Cole, R. V. Budny, J. S. deGrassie, W. W. Heidbrink, G. L. Jackson, M. J. Lanctot, R. Nazikian, H. Reimerdes, E. J. Strait, M. A. Van Zeeland, and DIII-D Rotation Physics Task Force, *Nucl. Fusion* **49**, 085005 (2009).
- ¹⁶W. M. Solomon, K. H. Burrell, A. M. Garofalo, S. M. Kaye, R. E. Bell, A. J. Cole, J. S. deGrassie, P. H. Diamond, T. S. Hahm, G. L. Jackson, M. J. Lanctot, C. C. Petty, H. Reimerdes, S. A. Sabbagh, E. J. Strait, T. Tala, and R. E. Waltz, *Phys. Plasmas* **17**, 056108 (2010).
- ¹⁷J. S. deGrassie, R. J. Groebner, K. H. Burrell, and W. M. Solomon, *Nucl. Fusion* **49**, 085020 (2009).
- ¹⁸J. S. deGrassie, J. E. Rice, K. H. Burrell, R. Groebner, and W. Solomon, *Phys. Plasmas* **14**, 056115 (2007).
- ¹⁹R. R. Dominguez and G. M. Staebler, *Phys. Fluids B* **5**, 3876 (1993).
- ²⁰O. D. Gurcan, P. H. Diamond, T. S. Hahm, and R. Singh, *Phys. Plasmas* **14**, 042306 (2007).
- ²¹Y. Camenen, A. G. Peeters, C. Angioni, F. S. Casson, W. A. Hornsby, A. P. Snodin, and D. Strintzi, *Phys. Rev. Lett.* **102**, 125001 (2009).
- ²²A. M. Garofalo, K. H. Burrell, J. C. DeBoo, J. S. deGrassie, G. L. Jackson, M. Lanctot, H. Reimerdes, M. J. Schaffer, W. M. Solomon, and E. J. Strait, *Phys. Rev. Lett.* **101**, 195005 (2008).
- ²³N. Smick, B. LaBombard, and C. S. Pitcher, *J. Nucl. Mater.* **337–339**, 281 (2005).
- ²⁴B. LaBombard, J. E. Rice, A. E. Hubbard, J. W. Hughes, M. Greenwald, J. Irby, Y. Line, B. Lipschultz, E. S. Marmor, C. S. Pitcher, N. Smick, S. M. Wolfe, S. J. Wukitch, and Alcator Group, *Nucl. Fusion* **44**, 1047 (2004).
- ²⁵W. M. Stacey, *Phys. Plasmas* **16**, 062505 (2009).
- ²⁶P. H. Diamond, C. J. McDevitt, O. D. Gurcan, T. S. Hahm, and V. Naulin, *Phys. Plasmas* **15**, 012303 (2008).
- ²⁷W. M. Stacey, *Phys. Plasmas* **18**, 102504 (2011).
- ²⁸W. M. Stacey, *Phys. Plasmas* **18**, 122504 (2011).
- ²⁹J. Luxon, *Nucl. Fusion* **42**, 614 (2002).
- ³⁰K. Miyamoto, *Nucl. Fusion* **36**, 927 (1996).
- ³¹C. S. Chang, S. Kue, and H. Weitzner, *Phys. Plasmas* **9**, 3884 (2002).
- ³²F. L. Hinton and M. Chu, *Nucl. Fusion* **25**, 345 (1985).
- ³³G. F. Matthews, G. Corrigan, S. K. Erents, W. Fundamenski, A. Kallenbach, T. Kurki-Suonio, S. Sipila, and J. Spence, JET Report EFDA-JET-CP902 01-02, 2002.
- ³⁴J. S. deGrassie, S. H. Mueller, and J. A. Boedo, *Nucl. Fusion* **52**, 013010 (2012).
- ³⁵J. Bodeo, J. deGrassie, B. Grierson, W. Solomon, W. Stacey, and D. Battaglia, *Phys. Plasmas* (in preparation).
- ³⁶T. E. Evans, K. H. Burrell, and M. E. Fenstermacher, *Phys. Plasmas* **13**, 056121 (2006).
- ³⁷W. M. Stacey and T. E. Evans, *Phys. Plasmas* **13**, 112506 (2006).
- ³⁸W. M. Stacey and T. E. Evans, *Nucl. Fusion* **51**, 013007 (2011).